

The saturation of N cycling in Central Plains streams: ^{15}N experiments across a broad gradient of nitrate concentrations

Jonathan M. O'Brien · Walter K. Dodds ·
Kymberly C. Wilson · Justin N. Murdock ·
Jessica Eichmiller

Received: 21 June 2006 / Accepted: 21 December 2006 / Published online: 23 March 2007
© Springer Science+Business Media B.V. 2007

Abstract We conducted $^{15}\text{NO}_3^-$ stable isotope tracer releases in nine streams with varied intensities and types of human impacts in the upstream watershed to measure nitrate (NO_3^-) cycling dynamics. Mean ambient NO_3^- concentrations of the streams ranged from 0.9 to 21,000 $\mu\text{g l}^{-1} \text{NO}_3^-$ -N. Major N-transforming processes, including uptake, nitrification, and denitrification, all increased approximately two to three orders of magnitude along the same gradient. Despite increases in transformation rates, the efficiency with which stream biota utilized available NO_3^- decreased along the gradient of increasing NO_3^- . Observed functional relationships of biological N transformations (uptake and nitrification) with NO_3^- concentration did not support a 1st order model and did not show signs of Michaelis-Menten type saturation. The empirical relationship was best described by a Efficiency Loss

model, in which log-transformed rates (uptake and nitrification) increase with log-transformed nitrate concentration with a slope less than one. Denitrification increased linearly across the gradient of NO_3^- concentrations, but only accounted for ~1% of total NO_3^- uptake. On average, 20% of stream water NO_3^- was lost to denitrification per km, but the percentage removed in most streams was <5% km^{-1} . Although the rate of cycling was greater in streams with larger NO_3^- concentrations, the relative proportion of NO_3^- retained per unit length of stream decreased as NO_3^- concentration increased. Due to the rapid rate of NO_3^- turnover, these streams have a great potential for short-term retention of N from the landscape, but the ability to remove N through denitrification is highly variable.

Keywords Denitrification · Nitrate · Nitrification · Saturation · Stream · Uptake

J. M. O'Brien · W. K. Dodds · K. C. Wilson ·
J. N. Murdock · J. Eichmiller
Division of Biology, Kansas State University,
232 Ackert Hall, Manhattan, KS 66506, USA

J. M. O'Brien (✉)
W.K. Kellogg Biological Station, Michigan State
University, 3700 E. Gull Lake Drive,
Hickory Corners, MI 49060-9516, USA
e-mail: obrien97@msu.edu

Global Institute of Sustainability, Arizona State
University, Tempe, AZ 85287-4501, USA

Introduction

Streams draining pristine watersheds typically export mostly organic nitrogen (N) and little dissolved inorganic N (Lewis 2002). Human land uses such as urbanization and fertilizing cropland can have large impacts on the concentrations of N transported in streams, particularly in the form of

nitrate (NO_3^-). Increased NO_3^- transport occurs in part because the concentrations in the water columns are raised well above levels typical of pristine watersheds (Bernot and Dodds 2005; Torrecilla et al. 2005). Increased N in flowing waters can interfere with biotic integrity of streams (Dodds and Welch 2000), as well as cause downstream eutrophication in marine habitats such as the Gulf of Mexico (Rabalais 2002).

In-stream processes influence the transport, retention, and removal of N from the landscape (Peterson et al. 2001; Mulholland 2004; Bernhardt et al. 2005). Within the context of larger river networks, low-order streams can have a disproportionately large impact on the rate at which N is retained and attenuated within streams (Alexander et al. 2000). N transport is governed in part by the rate of N cycling in the stream. Downstream transport is often referred to as N 'spiraling' due to the downstream displacement of N as it cycles from inorganic to organic forms and back again (Webster and Patten 1979).

Streams with short spiral length have relatively more short-term retention of N, while longer spiral lengths indicate less short-term retention. Long-term retention could be related to deposition of sediments over years or longer (Bernot and Dodds 2005) and will not be considered directly in this paper. Retention will be defined as short-term retention related to uptake processes for the purposes of our study.

Streams can also serve as an important site of denitrification (Hill 1979; O'Brien and Williard 2006), the process by which NO_3^- is converted to N_2 gas and nitrous oxide (N_2O) gas and constitutes a removal of biologically available N from the ecosystem. Denitrification (particularly the production of N_2) is of great interest to scientists because it is a permanent removal of N, as opposed to temporary retention within the stream channel. The production of N_2O via denitrification in streams is also of environmental concern, because N_2O is a powerful greenhouse gas and can catalyze stratospheric ozone destruction.

Prairie streams were historically common in central North America, but today a large portion of the native prairie landscape has been converted to agriculture and urban uses (Dodds et al. 2004). Fertilizer and pesticide application within

the watersheds has degraded the water quality of these formerly pristine prairie streams (Dodds and Oakes 2004). Human impacts on N retention in streams of this biome are relevant, because the areas historically covered with tallgrass prairie now contribute heavily to N transport into the Northern Gulf of Mexico (Alexander et al. 2000). We studied Central Plains streams under a range of anthropogenic N loadings to characterize spiraling and retention.

A lingering question, across all types of streams, is to what degree will anthropogenic increases in loading of dissolved N impact the transport, short-term retention and removal of N? Heterotrophic and autotrophic processes that influence in-stream spiraling of N are, in many instances, limited or co-limited by N and P (Tank and Dodds 2003; Niyogi et al. 2004). Nitrification and denitrification may be stimulated in N-rich agricultural sites, compared with N-poor prairie sites (Kemp and Dodds 2002a), and NO_3^- concentration can be the dominant predictor of denitrification in the sediments of agricultural streams (Inwood et al. 2005). Thus, increases in N concentration could result in greater retention or removal while increases in transport rates are negligible.

Bernot and Dodds (2005) argued that saturation of biological nutrient processing is inevitable under elevated nutrient concentrations because, at some point, other factors will begin to limit nutrient transformation rates. But phosphorus uptake or growth experiments in streams (Bothwell 1989; Mulholland et al. 1990) and lakes (Dodds 1995) reveal half-saturation constants for uptake or growth for assemblages that are far greater than those exhibited by individual organisms in laboratory culture. The rates of ammonium (NH_4^+) uptake, NO_3^- uptake, nitrification, and denitrification do not always saturate in prairie streams (Dodds et al. 2002; Kemp and Dodds 2002b). Furthermore, even if short-term increases in N cause saturation, the influence of chronic N increases is not well characterized across systems. Most uptake experiments have been conducted in streams with short-term spikes of nutrients, but less is known about uptake across streams that have had time to acclimate to higher nutrient concentrations (chronic N loading).

Functional relationships between N processing and concentration

There are three models we consider most likely to describe the relationship between N processing rates and N concentration, based on previously published relationships. Each model has distinct implications for the functional relationships between spiraling characteristics, such as spiral length and uptake velocity, and N concentration in the water column of the stream (Fig. 1).

The first model is a 1st order response, in which biological process rates are tightly linked to available NO_3^- and are directly proportional to N concentration. In the 1st order model, process

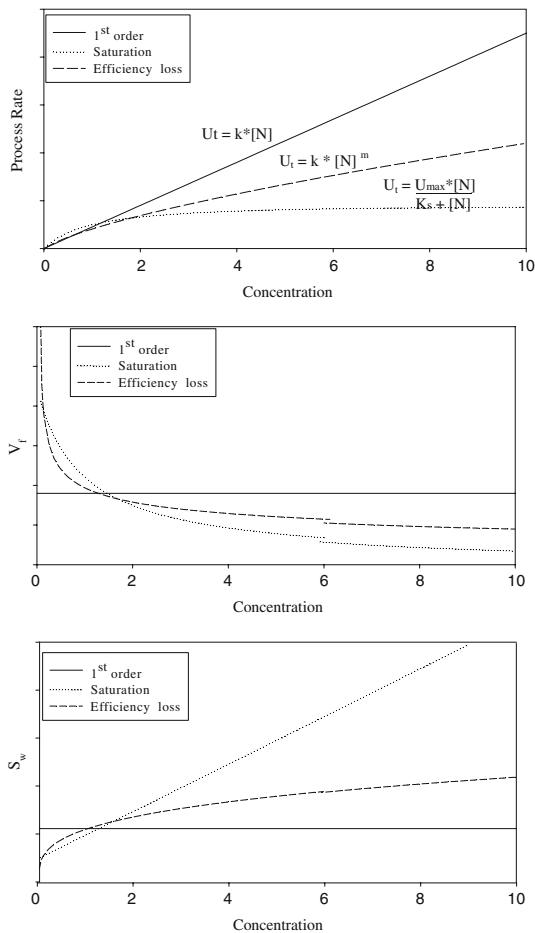


Fig. 1 Comparison of the three potential models of the relationship between stream N processing and concentration. Scales are linear

rates, such as uptake per unit area (U_t), nitrification, and denitrification, increase linearly with N concentration. Retention efficiency, as indexed by vertical uptake velocity (V_f) and uptake length (S_w), the average distance traveled before being taken up, are not expected to change in relation to increase in N load (Stream Solute Workshop 1990).

The second model takes the form of Michaelis–Menten uptake kinetics, and represents a clear saturation of processing rates as the supply of available NO_3^- exceeds biological demand (Bernot and Dodds 2005). In this model, U_t , nitrification and denitrification exhibit hyperbolic relationships, with increasing N concentration described by Michaelis–Menten type kinetics ($U_t = N \times U_{\max}/[k_s + N]$), where U_{\max} is the maximum rate of uptake, k_s is the half saturation coefficient, and N is the concentration of NO_3^-). As a result of saturation, S_w exhibits a linear increase with the increase in N load, whereas V_f would be expected to dramatically decrease along the same gradient.

In the third model, the rate of N cycling by the biota increases with N availability, but efficiency of the process rates relative to concentration declines. An example is the relationship between NH_4^+ uptake and concentration in streams observed by Dodds et al. (2002). This model is described by a power relationship in which the exponent (or order) is less than one ($U_t = k \times [N]^m$, where $m < 1$). We will refer to this model as Efficiency Loss model. The model predicts that process rates will increase with increasing N load, S_w will increase nonlinearly with increasing nutrient concentration, and V_f will decrease nonlinearly along the same gradient.

We used $^{15}\text{NO}_3^-$ stable isotope injections on a series of 9 streams with various human impacts, along a gradient of NO_3^- concentration (~ 1 – $20,000 \mu\text{g l}^{-1} \text{NO}_3^-$ -N), to characterize cycling and retention. The streams in our study varied widely, including undisturbed tallgrass prairie streams, incised silt-bottomed agricultural streams, and a concrete-lined urban ditch. The gradient of NO_3^- concentrations across the nine streams in this study allowed us to test the hypothesis that the rate of NO_3^- cycling within the stream would exhibit saturation with increasing NO_3^- concentrations.

Methods

Study sites

This study was conducted in the Flint Hills region of Northeast Kansas, USA, which is home to the largest tract of remaining tallgrass prairie in the Great Plains. The area is characterized by rolling hills that are underlain by limestone and shale layers (Oviatt 1998). Due to the shallow, rocky soils in much of the region, the primary land use in the area is cattle grazing, although deeper lowland soils are suitable for row crop agriculture. Nine streams in the vicinity of Manhattan, Kansas, were selected from among three general land use categories: prairie/reference, agriculture, and urban. Streams were all low order (first and second order), had low discharge, and varied widely in NO_3^- concentration (Table 1). The watershed characteristics of each of the streams are provided and are in order of increasing mean water column NO_3^- concentrations (Table 2).

Four streams draining native vegetation provided a baseline of human impact and nutrient concentrations. Kings Creek-K2A, Kings Creek-N4D, and Shane Creek are located on the Konza Prairie Biological Station. The watersheds drained by these streams are dominated by native tallgrass prairie. Natalie's Creek drains an unfertilized, annually burned cattle pasture of predominantly prairie grasses. Kings Creek (and N4D in particular) has been heavily studied, including descriptions of the N cycle (Dodds et al. 2000), aquatic community (Gray and Dodds 1998) and hydrology (Gray et al. 1998).

Two agriculturally influenced streams were also included in this study. Ag North Creek drains a watershed with mixed land uses flowing through a straightened, incised stream channel in a reach surrounded by row-crop agriculture. Swine Creek also flows through a straightened, incised stream channel and drains a mixed watershed, including row-crop agriculture and several livestock-rearing facilities. The riparian zones of both streams include grass buffer strips with occasional shrubs.

Additionally, three urban streams with varying levels of human impact were investigated. Little Kitten Creek drains a watershed dominated by a

Table 1 Chemical and hydrologic parameters of the nine streams in this study during the $^{15}\text{NO}_3^-$ addition experiments

Stream name	Date of experiment	NO_3^- ($\mu\text{g l}^{-1}$)	NH_4^+ -N ($\mu\text{g l}^{-1}$)	DON ($\mu\text{g l}^{-1}$)	SRP ($\mu\text{g l}^{-1}$)	Hypohreic NO_3^- -N ($\mu\text{g l}^{-1}$)	Q (l s^{-1})	Width (m)	Depth (m)	Velocity (m min^{-1})	A _j /A	A (10^{-3} s^{-1})
Kings Creek-K2A	June 2004	0.9	6.7	85	1.9	8	26.3	2.5	0.09	6.7	1.34	5.46
Shane Creek	May 2005	1.2	4.7	98	1.0	4	4.4	2.36	0.08	1.3	0.50	0.20
Natalie's Creek	June 2004	6.0	3.1	156	2.4	8	1.3	1.2	0.04	1.6	NA	NA
Kings Creek-N4D	May 2003	8.6	0.0	196	0.5	10	13.4	2.4	0.07	5.0	0.09	0.02
Ag North	June 2003	35	31.7	111	0.2	456	0.2	0.77	0.02	1.1	0.06	0.19
Little Kitten Creek	June 2005	168	24.2	159	7.2	180	20.1	3.25	0.14	2.7	0.13	0.35
Wal-Mart Ditch	May 2004	277	28.3	472	35.4	NA	1.6	2.1	0.05	0.9	NA	NA
Campus Creek	June 2003	2900	7.8	N.D.	4.0	808	2.9	2.56	0.08	0.9	0.07	0.17
Swine Creek	June 2005	21000	3.3	N.D.	15.5	17000	5.4	1.57	0.07	2.8	0.23	0.36

NA = data not available

Table 2 Location, watershed characteristics, and stream channel characteristics of the streams in this study

Stream name	Latitude, longitude	%Native vegetation	%Row-crop agriculture	%Urban	Burn frequency	Livestock grazing	%Stream shading	Reach length (m)	Stream-bed characteristics
Kings Creek-K2A	39°06.008' N, 96°34.454' W	100	0	0	2 year	No	37	180	Cobble/bedrock
Shane Creek	39°06.779' N, 96°33.220' W	100	0	0	1 year	No	57	300	Cobble
Natalie's Creek	39° 13.723' N, 96° 39.530' W	100	0	0	1 Year	Yes	44	200	Cobble/bedrock
Kings Creek-N4D	39° 05.271' N, 96° 35.067' W	100	0	0	4 year	Yes	39	125	Cobble
Ag North Creek	39° 12.741' N, 96° 35.584' W	25	30	45	NA	Yes	0	200	Silt/clay
Little Kitten Creek	39°12.361' N, 96° 36.083' W)	0	0	100	NA	NA	76	270	Cobble
Wal-Mart Ditch	39° 11.135' N, 96° 33.500' W	8	0	92	NA	NA	0	300	Concrete
Campus Creek	39° 11.577N 96° 34.722' W	0	0	100	NA	NA	71	125	Cobble/sand/clay
Swine Creek	39° 13.181' N, 96° 35.271' W	30	34	36	NA	Yes	11	1000	Silt/clay

Burn frequency and livestock grazing refer to land-management practices in the native vegetation portions of the watershed. Stream shading refers to shading due to riparian vegetation. Reach length refers to the distance between the 15 N injection site and the last water sampling station

golf course (that has retained a portion of native vegetation) and recent housing development. Campus Creek drains a watershed on the campus of Kansas State University and exhibits elevated NO_3^- concentrations that probably originate from historic livestock holding facilities (now paved, with buildings, or with lawns) upstream from the point of the experiment. Finally, Wal-Mart Ditch is a former channel of the Big Blue River and is fed by the storm drainage system of the City of Manhattan, Kansas. The stream has been channelized and landscaped with 2 m high retaining walls on either side and the streambed is sealed with concrete.

Field methods

$^{15}\text{NO}_3^-$ isotope addition experiments were conducted on each of the streams between May 2003 and June 2005 as part of the Lotic Inter-site Nitrogen eXperiment II (LINX II) project. A solution of $^{15}\text{NO}_3^-$, along with a NaBr conservative solute, was injected into the stream at a

steady rate (20 ml min^{-1}) for 24 h. The amount of K^{15}NO_3 added to the release solution was scaled for each individual stream to produce a target δ enrichment of 20,000‰ of the NO_3^- in the stream water (Mulholland et al. 2004).

Pre-enrichment stream water samples (duplicate samples for $^{15}\text{NO}_3^-$) were collected to establish background isotopic ratios at six stations along the length of the stream reach before the release. Background samples of dissolved $^{15}\text{N}_2$ and $^{15}\text{N}_2\text{O}$ were also collected at 10 stations along the length of the reach before the release.

During the $^{15}\text{NO}_3^-$ release, duplicate samples for $^{15}\text{NO}_3^-$ analysis were collected at six stations along the length of the reach (approximately 300 m) at 01:00 of the second day (12 h after the release began) and 12:00 of the second day (23 h after the release began) to determine day and night N uptake and spiraling metrics. Samples were filtered in the field through Whatman GF/F glass fiber filters ($0.7 \mu\text{m}$ retention) and transported back to the laboratory where they were frozen or analyzed immediately.

Samples of dissolved gaseous N were collected at 10 locations along the length of the reach during the $^{15}\text{NO}_3^-$ releases coincident with water sampling. Water samples were collected in 60-ml (2003) or 140-ml (2004 and 2005) plastic syringes fitted with stopcocks, with care taken not to include bubbles with the samples. With the sample syringe submerged underwater, 20 ml of high purity He were added to each syringe. Syringes containing both He and stream water were shaken for 5 min to allow equilibration of dissolved N_2 gas into the He headspace. Again underwater, stream water was expelled from the syringes, and He headspace was collected in evacuated 12-ml exetainer vials (Vial Type 3, Labco, High Wycombe, Buckinghamshire, UK). The sample vials were stored in water-filled centrifuge tubes to avoid contamination from the atmosphere, and were analyzed for $^{15}\text{N}_2$ and $^{15}\text{N}_2\text{O}$ by mass spectrometry (Mulholland et al. 2004; SK Hamilton unpublished).

Samples of hyporheic water were collected along the length of the stream reach with a “sipper” sampler. The “sipper” consisted of a hollow aluminum tube with a 1.25-cm² opening near the tip containing a 1.5-mm inner diameter TFE tube with a stainless steel 0.3-mm mesh fuel filter at the end (SK Hamilton personal communication). The tip of the “sipper” was inserted 7–19 cm into the substratum and the sample was collected via syringe, after rinsing the tubing and bottle with hyporheic water. Hyporheic water samples were collected at each water sampling station (six samples per stream), placed on ice during transport, filtered with 0.45- μm nylon filters, and analyzed for NO_3^- .

Standing-stock organic biomass for each stream was measured 24 h after the release, at 10 stations along the reach. At each station, a 1-m² metal frame was placed randomly in the stream channel, and all coarse benthic organic matter (CBOM), macrophytes, and filamentous algae found within the frame were collected. Surface (material suspended with gentle agitation of water above the benthic surface) and deep (material from the surface to several cm deep suspended into the water with vigorous stirring) fine benthic organic matter (FBOM) were collected using a stovepipe corer device.

Epilithic biofilm samples were collected by scraping a known surface area from three rocks selected without bias from each sampling station. Additional biomass samples were collected at each of the six water-sampling stations for ^{15}N analysis using the same techniques as biomass sampling.

Yellow Springs Instruments logging data sondes were deployed within the reach to take continuous (5-min interval) dissolved O_2 measurements for the duration of the ^{15}N experiments. These data were used to calculate whole stream metabolism, community respiration (CR), and gross primary production (GPP), using the one-station method (Bott 1996). Either propane or acetylene was used as a gas tracer, in conjunction with NaBr as a conservative hydraulic tracer, to determine the rate of reaeration along the stream reach. Gas was directly bubbled into the stream, along with a concurrent NaBr addition (to correct for dilution of gas). Water and dissolved-gas samples were taken at several locations downstream. Dissolved-gas samples were collected by drawing 5 ml of stream water into a 10-ml plastic syringe and transferring the water into a 15-ml He-filled exetainer.

Water samples were analyzed for bromide concentration using an ion-selective electrode. Dissolved gas samples were analyzed for propane and acetylene using a Shimadzu GC-14A gas chromatograph with a flame-ionization detector (Hayesep Q column, oven temperature = 50°C, flow rate 25 ml/min). The dilution-corrected decline in propane or acetylene concentration was then used to calculate the longitudinal gas-exchange coefficient. This coefficient was then multiplied by a correction factor of 1.39 for propane (Rathbun et al. 1978) or 0.867 for acetylene to convert it to an O_2 exchange rate. Average velocity of the stream was then multiplied by the longitudinal O_2 exchange coefficient to determine the time-based reaeration coefficient (K_{20}).

The channel hydrologic parameters and transient storage zone sizes for each stream were measured using a step release of a hydrologically conservative tracer (NaBr) into the stream (Webster and Ehrman 1996). Stream Br^- concentrations were measured over time at a downstream

station. The shape of the Br^- pulse at the downstream site was used to quantify the size of the transient storage zone using the OTIS-P model (Stream Solute Workshop 1990).

Laboratory methods

The ^{15}N content of stream water NO_3^- was determined by using a modified version of the method presented by Sigman et al. (1997). Stream water samples of about $50 \mu\text{g NO}_3^-$ -N were concentrated and NH_4^+ was removed by adding 3.0 g MgO and 5.0 g NaCl and boiling. Stream water $^{15}\text{NO}_3^-$ samples collected during the isotope release were spiked with additional NO_3^- ($10\times$ stream water NO_3^- concentration) in order to reduce $\delta^{15}\text{N}$ below $2,000\text{‰}$ (the upper detection limit of the stable isotope laboratory). Samples were then transferred to 250-ml media bottles to which an additional 0.5 g MgO, 0.5 g Devarda's Alloy, and a Teflon filter packet were added. The Teflon filter packet was constructed by sealing a 10-mm Whatman GF/D glass-fiber filter, acidified with $25 \mu\text{l}$ of 2.0 M KHSO_4 , within a packet made of a folded piece of 2.5-cm Teflon plumbing tape. The sample NO_3^- was reduced to NH_4^+ by reacting at 60°C for 48 h with DeVarda's alloy. Sealed bottles were then placed on a shaker for 7 days to allow for diffusion. The hydrophobic Teflon allowed for diffusion of NH_3 onto the acidified filter. The glass-fiber filter was then removed from the media bottle, dried, and analyzed for ^{15}N on a ThermoFinnigan Delta Plus mass spectrometer with a CE 1110 elemental analyzer and a ConFlo II interface.

Stream water NO_3^- concentration was determined colorometrically by using the cadmium reduction method on a Technicon auto-analyzer (APHA 1995). Stream water NH_4^+ concentration was analyzed by using the indophenol method on a Technicon auto-analyzer. Stream water-soluble reactive phosphorus (SRP) was determined with the molybdate reduction method and analyzed on a Technicon auto-analyzer (APHA 1995). Total dissolved N (TDN) and total dissolved P (TDP) were determined by using a persulfate digestion, followed by analysis for NO_3^- or SRP, respectively (Valderrama 1981). Br^- hydraulic tracer

concentrations were determined with a calibrated Orion 9435BN ion-specific electrode.

Standing-stock biomass was oven dried at 60°C and weighed. Subsamples were ashed at 450°C for 1.5 h to determine the percentage of organic matter. Biomass samples for ^{15}N analysis were freeze-dried, ground, and analyzed for ^{15}N on a ThermoFinnigan Delta Plus mass spectrometer with a CE 1110 elemental analyzer and a ConFlo II interface.

Calculations

Data from the plateau stream water $^{15}\text{NO}_3^-$ samples were corrected for background and spike $^{15}\text{NO}_3^-$ to determine total concentration of tracer $^{15}\text{NO}_3^-$ at each station. $^{15}\text{NO}_3^-$ concentration was then multiplied by discharge at each station to find the total $^{15}\text{NO}_3^-$ flux. Station-specific discharge was calculated by dilution of the Br^- hydraulic tracer. The flux of $^{15}\text{NO}_3^-$ at each station was ln-transformed, and slope of the decline in ln-transformed $^{15}\text{NO}_3^-$ flux over the length of the reach (k_m) was calculated using linear regression.

We calculated uptake length (S_w), from slope, k_m , as

$$S_w = -1 \times k_m^{-1} \quad (1)$$

for $^{15}\text{NO}_3^-$ during both plateaus measured at each stream. From S_w , we calculate the uptake rate (U_t):

$$U_t = \frac{F}{S_w \times w} \quad (2)$$

in which F is the flux of NO_3^- in stream water and w is average width of the stream. In this capacity, U_t accounts for total $^{15}\text{NO}_3^-$ uptake, and includes assimilation and denitrification. Mass transfer coefficient (V_f) was then calculated as

$$V_f = \frac{U_t}{C} \quad (3)$$

in which C is the concentration of NO_3^- in the stream water (Stream Solute Workshop 1990).

The rate of nitrification occurring within the stream reach was calculated by mass balance of

NO_3^- entering and leaving the reach. NO_3^- concentration was multiplied by discharge at stations 1 (most upstream) and 6 (most downstream) below each $^{15}\text{NO}_3^-$ addition site to achieve influx (IN) and out flux (OUT) rate measurements, respectively, of NO_3^- in each experimental stream reach. Groundwater NO_3^- flux rate (GW) inputs were calculated based on the change in stream discharge (Q) between stations 1 and 6, multiplied by average hyporheic NO_3^- concentration. Uptake flux (U) was calculated by multiplying U_t (which includes denitrification and assimilative uptake) by the stream width and reach length. Nitrification was then calculated as the difference of inputs and outputs from the stream reach according to the mass balance equation:

$$\text{Nitrification} = \text{IN} + \text{GW} - U - \text{OUT} \quad (4)$$

The rate of denitrification occurring within the stream was determined by using longitudinal flux of tracer $^{15}\text{N}_2$ with the model presented by Mulholland et al. (2004). Flux of total $^{15}\text{N}_2$ was calculated by multiplying the mole fraction of ^{15}N in the N_2 gas at each station during the $^{15}\text{NO}_3^-$ experiment by the measured mass of dissolved N_2 in the water, multiplied by the stream discharge. Tracer $^{15}\text{N}_2$ was then calculated by correcting total $^{15}\text{N}_2$ for background by subtracting ambient $^{15}\text{N}_2$ flux as measured from the pre- ^{15}N addition samples. The concentration of dissolved N_2 was assumed to be at atmospheric saturation for the calculation of denitrification. This assumption was verified based on N_2 mass measurements provided by the stable Isotope spectrometry laboratory.

The pattern of the longitudinal $^{15}\text{N}_2$ flux was then used to determine the coefficient of denitrification (K_{den}) by using the equation:

$$dN_2/dx = K_{\text{den}} \times A_o \times e^{-(k_m) \times x - k_2 \times N_2} \quad (5)$$

in which N_2 is flux of tracer $^{15}\text{N}_2$ ($\mu\text{g s}^{-1}$), A_o is $^{15}\text{NO}_3^-$ flux at the injection location, k_m is loss rate of $^{15}\text{NO}_3^-$ with distance (inverse of S_w), k_2 is N_2 air-water gas exchange coefficient, and x is downstream distance. Estimates of K_{den} (m^{-1}) was then calculated using an iterative approach that minimized the sum of squares between modeled and observed $^{15}\text{N}_2$ fluxes by using the

Microsoft Excel Solver tool (Microsoft Excel 2000, Microsoft Corporation, Redmond, WA). The rate of denitrification as N_2 ($\mu\text{g N m}^{-2} \text{s}^{-1}$) was calculated by multiplying stream NO_3^- flux by K_{den} and dividing by average stream width. This same model was used to measure the rate of $^{15}\text{N}_2\text{O}$ production. Total denitrification was calculated as the sum of the rates of $^{15}\text{N}_2$ and $^{15}\text{N}_2\text{O}$ production. The percent of NO_3^- flux removed per km of stream length was calculated based on the K_{den} using the equation:

$$\% \text{Removal} = (1 - e^{K_{\text{den}} \times 1000}) \times 100 \quad (6)$$

Assimilatory uptake by biomass was calculated for each biomass compartment in the stream, based on total mass of ^{15}N tracer found in each biomass compartment (e.g., surface and deep FBOM, epilithon, leaves) at each station. Biomass-specific uptake was calculated as total molar mass of ^{15}N tracer per m^2 of each compartment divided by mole frequency of ^{15}N to ^{14}N in the NO_3^- of the overlying stream water.

Biological N demand was calculated for each stream according to the method and assumptions of Webster et al. (2003). Autotrophic demand was calculated for each stream, based on GPP measurements from stream metabolism estimates. Net primary production was estimated to be 70% of GPP (Graham et al. 1985; Hill et al. 2001). Photosynthetic quotient, or number of moles of CO_2 fixed per mole of O_2 released, was estimated to be 1.2 (Wetzel and Likens 2000). A carbon to nitrogen (C:N) molar ratio of 12 was then used to calculate N demand from CO_2 fixed. This ratio is the C:N of actively growing algal cultures, instead of measured C:N of the stream epilithon, which contains non-algal materials.

Heterotrophic N demand was then calculated using CR from the metabolism estimates (Webster et al. 2003). CR was corrected for autotrophic respiration (30% of GPP) and nitrification (2 mol $\text{O}_2/\text{mol N}$) to determine heterotrophic respiration. A respiratory quotient of 0.85 was used to convert number of moles O_2 consumed to number of moles CO_2 evolved. Heterotrophic production was then assumed to be 28% of heterotrophic respiration, based on CO_2 evolution.

Heterotrophic biomass was assumed to have a molar C:N of 5. Actual C:N of FBOM at each stream was used to calculate the proportion of heterotrophic N demand satisfied by consumption of FBOM. Total biotic N demand was the sum of autotrophic and heterotrophic N demand calculated from whole-stream metabolism measurements.

Statistical analyses

Linear regression was used to test for a relationship between stream metabolism and transient storage zone size. An ANCOVA procedure was used to detect any consistent effect of day and night on NO_3^- spiraling metrics and process rates, with NO_3^- concentration used as the continuous covariate. All variables in the ANCOVA were similarly log transformed. Ratios of U_i :nitrification were tested against a mean of 1 for day and night samplings by using a paired t -test.

Models of biotic response to increasing NO_3^- concentration were evaluated using the following statistical tests. The relationship between process rate and NO_3^- concentration was considered to be saturated if there was a significant fit with the Michaelis–Menten model (using least squares regression with Levenberg–Marquardt estimation algorithm, and non-log transformed data) and calculated K_s was within the range of experimental NO_3^- concentrations in the study. Linear regression was used to determine 1st order and Efficiency Loss models ($df = 9$ unless otherwise stated). In these regression analyses, dependent and independent variables were log transformed to satisfy regression assumptions of constant residual variance and normality of residuals and to reduce leverage effects of high- NO_3^- streams. Due to the log-transformations, the slope of any 1st order relationship between dependent and independent variables would be equal to 1, which was determined using a t -test of the slope of the regression ($H_a:m = 1$). If the Efficiency Loss model was valid, then the slope of the regression would have to be between zero and one ($0 < m < 1$), which was likewise tested using t -tests ($H_a:m < 1$). Saturation was also tested using S_w by linear regression between S_w and stream NO_3^- concentration, in which the

Michaelis–Menten model would be valid if there was a linear relationship between S_w and mean stream NO_3^- concentration, the 1st order model would be valid no relationship existed between S_w and mean stream NO_3^- , or the Efficiency Loss model would be valid if as significant power relationship was found in which $m < 1$. These relationships were tested using linear regression of non-log-transformed variables (linear relationship) and log-transformed variables (power relationship) with a t -test of the slope estimate. Censored regression (such as Tobit regression) was not used because of the small sample size, which may bias the maximum likelihood estimation that forms the basis of such techniques (Helsel and Hirsch 2002). All statistical tests were conducted with Statistica 6 (Statsoft, Tulsa, OK, USA) software package.

Results

Stream chemical and physical parameters

Chemical and hydrologic conditions differed widely across the streams (Table 1). Nitrate concentration ranged across five orders of magnitude, from 0.9 to 21,000 $\mu\text{g l}^{-1}$ NO_3^- -N. Concentrations of NH_4^+ ranged from below the detection limit ($1.0 \mu\text{g l}^{-1}$) to 32 $\mu\text{g l}^{-1}$ NH_4^+ -N, and dissolved organic N concentration ranged from 85 $\mu\text{g l}^{-1}$ to 472 $\mu\text{g l}^{-1}$ -N. Organic N was the dominant N fraction in low nutrient streams, whereas NO_3^- was the largest component in high NO_3^- streams (DON could not be detected in Campus Creek and Swine Creek using the presulfate-digestion method due to high background NO_3^- concentrations). Soluble reactive phosphorus concentrations ranged from 0.2 to 35.4 $\mu\text{g l}^{-1}$. Hyporheic NO_3^- concentrations tended to be similar to stream NO_3^- concentrations, and usually ranged within an order of magnitude of the mean. The hyporheic NO_3^- concentration at Natelie's creek (mean = 8.4 $\mu\text{g l}^{-1}$) ranged from 3.6 to 17 $\mu\text{g l}^{-1}$, while Swine creek (mean = 16,000 $\mu\text{g l}^{-1}$) ranged from 2,400 to 35,000 $\mu\text{g l}^{-1}$.

All streams in this study were low-order, shallow and had discharges of 0.2–26.3 l s^{-1} .

Average water velocities ranged from 0.9 to 6.7 m min⁻¹. The relative size of transient storage zones (A_s/A , the ratio of transient storage zone area to stream channel area) also differed across streams, ranging from 0.06 in the channelized reach of Ag North to 1.34 in the natural prairie reach of Kings Creek-K2A. Exchange rates of these transient storage zones (α) differed across streams but were not correlated with size of the transient storage zone. We were unable to obtain estimates of transient storage for Natalie's Creek or Wal-Mart Ditch, due to flow disruptions that occurred during the conservative tracer release.

Stream metabolism and biomass

Whole-stream estimates of metabolism demonstrated that many of the streams had a strong autotrophic component (Table 3). Gross primary production (GPP) ranged from 0.62 g O₂ m⁻² day⁻¹ in Natalie's Creek to 12.5 g O₂ m⁻² day⁻¹ in Wal-Mart Ditch. Many of the streams were not shaded, leading to significant growths of filamentous algae, macrophytes, and epilithon. Community respiration ranged from -0.97 g O₂ m⁻² day⁻¹ at Campus Creek to -7.02 g O₂ m⁻² day⁻¹ at Wal-Mart Ditch. The GPP and CR did not significantly co-vary along the gradient of increasing stream NO₃⁻ concentration. There was no statistically significant relationship ($P = 0.98$) between CR and the cross-sectional area of transient storage zone (A_s), as would be true if community respiration rates measured by O₂ changes in the water column were driven by activity within the hyporheic zone of these streams.

Surface and deep (0–10 cm) FBOM tended to be the largest standing-stock compartments across streams (Fig. 2). The exception to this was Wal-Mart Ditch, in which the thick algal biofilm was classified as epilithon and was the only biomass compartment found in the stream in substantial amounts. None of the standing-stock biomass compartments seemed to increase along the gradient of increasing NO₃⁻ concentration.

Nutrient dynamics

Nitrate uptake lengths (S_w) ranged from 17 m in Shane Creek to 2,800 m in Little Kitten Creek, and became longer along the increasing NO₃⁻ gradient (Fig. 3). There was large diurnal variability in S_w between the midnight and noon sampling, but the diurnal effect was not consistently greater in either day or night sampling across streams (ANCOVA, NO₃⁻ as covariate, $F_{1,15} = 0.17$, $P = 0.69$). The efficiency of NO₃⁻ utilization, as indexed by V_f , decreased along the gradient of increasing NO₃⁻ (Fig. 3).

Nitrate uptake rates ranged from 0.01 μg N m⁻² s⁻¹ in Shane Creek to 192 μg N m⁻² s⁻¹ in Swine Creek, and increased along the gradient of streams with increasing NO₃⁻ concentration (Fig. 3). Nitrification ranged from 0.01 μg N m⁻² s⁻¹ at Kings Creek-K2A to 59.2 μg N m⁻² s⁻¹ at Swine Creek (Fig. 3). Nitrification increased with greater NO₃⁻ concentration in a similar manner to U_t . Nitrification and U_t were essentially balanced in the nine streams of this study, despite the dual increases in process rates that occurred along the NO₃⁻ gradient (Fig. 4). In addition, diurnal changes in uptake and nitrification often shifted the balance between U_t

Table 3 Whole-stream metabolism estimates during ¹⁵NNO₃⁻ release at each of the streams

GPP: gross primary production; CR: community respiration. $P:R$ is the ratio of production to respiration. The O₂ exchange coefficient is the rate at which dissolved O₂ exchanges with the atmosphere

Stream	GPP (g O ₂ m ⁻² day ⁻¹)	CR (g O ₂ m ⁻² day ⁻¹)	$P:R$ ratio	O ₂ exchange coefficient (×10 ⁻³ min ⁻¹)
Kings Creek-K2A	2.0	-3.6	0.5	18.9
Shane Creek	7.0	-6.2	1.1	18.0
Natalie's Creek	0.6	-2.7	0.2	24.5
Kings Creek-N4D	6.2	-3.9	1.6	25.2
Ag North	3.2	-2.7	1.2	5.1
Little Kitten Creek	4.3	-4.2	1.0	12.8
Wal-Mart Ditch	12.5	-7.0	1.8	18.5
Campus Creek	1.0	-1.0	1.0	1.6
Swine Creek	2.7	-4.4	0.6	9.2

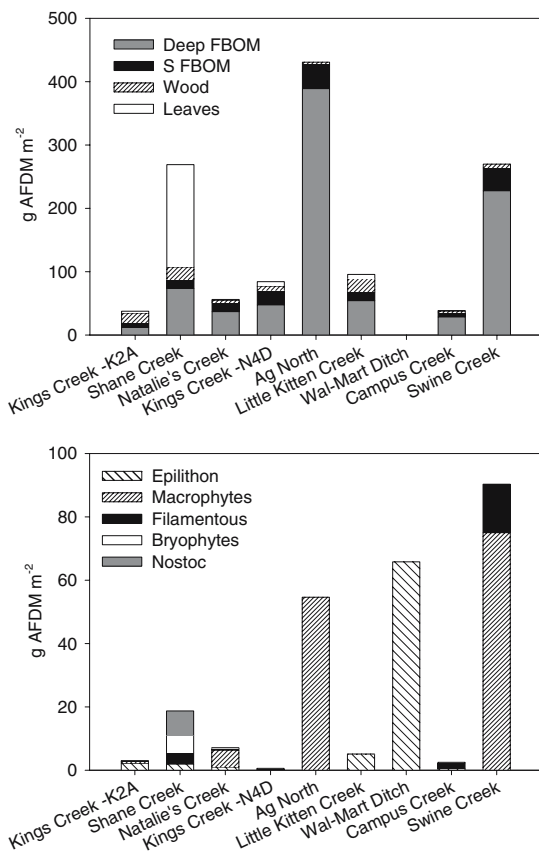


Fig. 2 Average standing-stock organic matter compartments across the streams in this study

and nitrification. These ratios of U_t :nitrification did not significantly differ from one during either day or night samplings.

Total denitrification ranged from below detection to $2.0 \mu\text{g N m}^{-2} \text{s}^{-1}$ in Swine Creek (Fig. 5). Isotopic tracer was not detected in dissolved N_2 in Shane Creek, Ag North and Kings Creek-K2A, nor in dissolved N_2O in Shane Creek and Kings Creek-K2A. The total denitrification rates were greater at night than in the day in all of the high- NO_3^- streams. In nearly all of the streams, the dominant end product of denitrification was N_2 gas (Table 4). Production of N_2O in most cases was $<1\%$ for total denitrification. The exception to this was Ag North, in which there was no detectable $^{15}\text{N}_2$ production, while there was a relatively low N_2O production. With higher background concentration of N_2 , the detection limit for denitrification with N_2 as the end product still exceeded N_2O production rate in this stream.

Nutrient dynamics in relation to NO_3^- concentration

The largest and most important gradient across the nine streams in this study was NO_3^- concentration, which allowed us to test the hypothesis that the rate of NO_3^- cycling within the stream would exhibit saturation with increasing NO_3^- concentrations. The statistical parameters used to test the criteria of the three functional relationship models can be found in Table 5.

We found a significant Michaelis–Menten model fit to the relationship between U_t and NO_3^- , however, the half-saturation coefficient was several orders of magnitude higher than experimental concentrations ($K_s = 1.9 \times 10^{10} \mu\text{g l}^{-1} \text{NO}_3^- \text{N}$), suggesting that there was no saturation occurring within the broad range of concentrations encountered in this study. The high statistical significance of this Michaelis–Menten model was due to the high degree of leverage by the Swine Creek data. This leveraging was not an issue with log-transformed data. We found a significant log–log relationship ($R^2 = 0.84$, $P < 0.001$) between $\log U_t$ and $\log \text{NO}_3^-$ (Fig. 6) with a slope of 0.66 (SE = 0.11). The slope of this relationship was significantly different from a slope 1, which excludes the 1st order model. The Efficiency Loss model fit both required criteria ($m < 1$, $m > 0$).

The relationship between nitrification and NO_3^- concentration yielded significant Michaelis–Menten model fit, but due to a very large K_s relative to experimental concentrations ($K_s = 4.0 \times 10^{10} \mu\text{g l}^{-1} \text{NO}_3^- \text{N}$), no saturation of nitrification across the gradient of streams concentrations was evident. We found a significant relationship ($R^2 = 0.62$, $P = 0.012$) between \log nitrification and $\log \text{NO}_3^-$ concentration across the streams in this study (Fig. 6) with a slope of 0.54 (SE = 0.16). The slope of this regression was significantly different from a slope 1, which would have been true if the 1st order model were valid. The Efficiency Loss model fit both required criteria ($m < 1$, $m > 0$).

Log-transformed total denitrification demonstrated a marginally significant linear relationship with $\log \text{NO}_3^-$ concentration ($R^2 = 0.54$, $df = 7$, $P = 0.061$) (Fig. 7). Although there was no

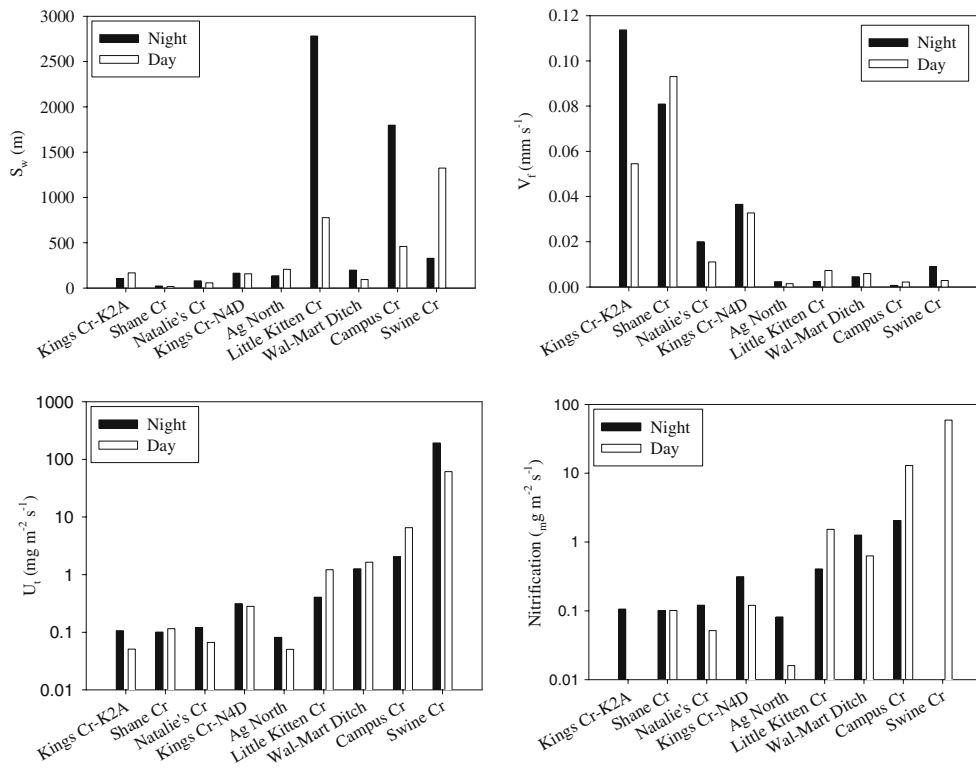


Fig. 3 Nitrate spiraling parameters and nitrification in day and night across the nine streams in this study. Streams are in order of increasing nitrate concentration

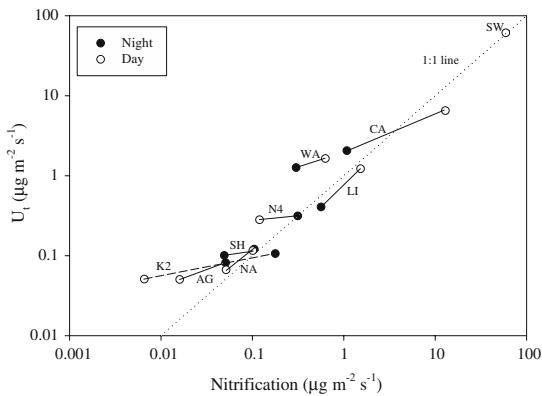


Fig. 4 Relationship between uptake and nitrification for the nine streams in this study. Points to the left of the dotted 1:1 line represent greater uptake than nitrification. The paired day and night uptake and nitrification points are linked with a solid line and are designated by the stream name: Kings Cr.-K2A: K2 (connecting line dashed), Shane Cr.: SH, Natalie's Cr.: NA, Kings Cr.-N4D: N4, Ag North: AG, Little Kitten Cr.: LI, Wal-Mart Ditch: WA, Campus Cr.: CA, Swine Cr.: SW

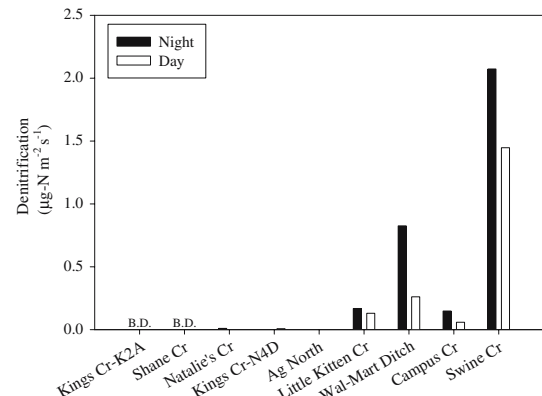


Fig. 5 Denitrification in day and night samplings. Denitrification in Kings Creek-K2A and Shane Creek were below detection (BD)

Table 4 Rates of denitrification observed in the nine streams, listed in order of increasing NO_3^- concentration

	Total denitrification ($\text{mg N m}^{-2} \text{ day}^{-1}$)	N_2 production ($\text{mg N m}^{-2} \text{ day}^{-1}$)	N_2O production ($\mu\text{g N m}^{-2} \text{ day}^{-1}$)	Percent removed (% km^{-1})
Kings Creek-K2A	0.0	0.0 ^a	0.0 ^a	0
Shane Creek	0.0	0.0 ^a	0.0 ^a	0
Natalie's Creek	0.6	0.6	0.5	66
Kings Creek-N4D	0.2	0.2	0.4	5
Ag North	0.0	0.0 ^a	0.4	0
Little Kitten Creek	12.8	12.8	55	13
Wal-Mart Ditch	43.6	43.6	27	91
Campus Creek	8.8	8.4	360	3
Swine Creek	221	219	2370	3

N_2O production due to denitrification composed only a small proportion of the total denitrification occurring in the streams, and is presented in smaller units than those for N_2 production. Percent removed is the cumulative removal of NO_3^- by denitrification, as a proportion of initial flux, over 1 km

^a Below detection

Table 5 Statistical parameters used to test the criteria of the three functional relationship models

Model:	Michaelis–Menten			Log–log regression				
	R^2	P	K_s	R^2	P	m (SE)	T ($m = 1$)	P
Parameter:								
U_t	0.99	<0.001	1.9×10^{10}	0.84	<0.001	0.66 (0.11)	3.12	0.012
Nitrification	0.99	<0.001	4.0×10^{10}	0.62	0.012	0.54 (0.16)	2.88	0.018
Denitrification	0.99	<0.001	1.4×10^9	0.54	0.061	0.87 (0.36)	0.36	0.74

evidence for saturation, the slope of the relationship was not significantly distinguishable from 1 and marginally distinguishable from zero, therefore the relationship fits the criteria for the 1st order model. Denitrification estimates from Kings Creek-K2A and Shane Creek were excluded from this analysis because denitrification could not be detected in these streams. The denitrification velocity (V_{den}) did not have a significant relationship with nitrate concentration. Production of N_2O by denitrification was also related to NO_3^- concentration ($R^2 = 0.93$, $df = 7$, $P < 0.001$). The ratio of $\text{N}_2\text{O}:\text{N}_2$ production did not significantly change along the NO_3^- gradient.

A significant relationship ($R^2 = 0.60$, $P = 0.013$) existed between $\log S_w$ and $\log \text{NO}_3^-$ concentration across the streams in this study, indicating that the average distance traveled by NO_3^- increased as the quantity of NO_3^- increased (Fig. 6). Linear regression of non-transformed S_w and NO_3^- concentration did not yield a significant relationship ($R^2 = 0.19$, $P = 0.23$). Uptake lengths also tend to be heavily influenced by the other factors such as discharge, which can be taken into

account by examining stream NO_3^- flux (concentration $\times Q$). The relationship between $\log S_w$ and $\log \text{NO}_3^-$ flux was significant ($R^2 = 0.74$, $P = 0.003$).

The final NO_3^- cycling characteristic that we tested was V_f , which can be used as an index of the efficiency of uptake relative to the available NO_3^- . Again, if saturation were occurring as predicted by the Michaelis–Menten model, we would expect V_f to decrease in relation to NO_3^- concentration. We found a significant negative linear relationship ($R^2 = 0.58$, $P = 0.017$) between $\log V_f$ and $\log \text{NO}_3^-$ concentration across the streams in this study (Fig. 6).

Discussion

The relationship between spiraling and concentration

The goal of this study was to determine the influence of N concentration on in-stream N processing across a wide variety of stream types

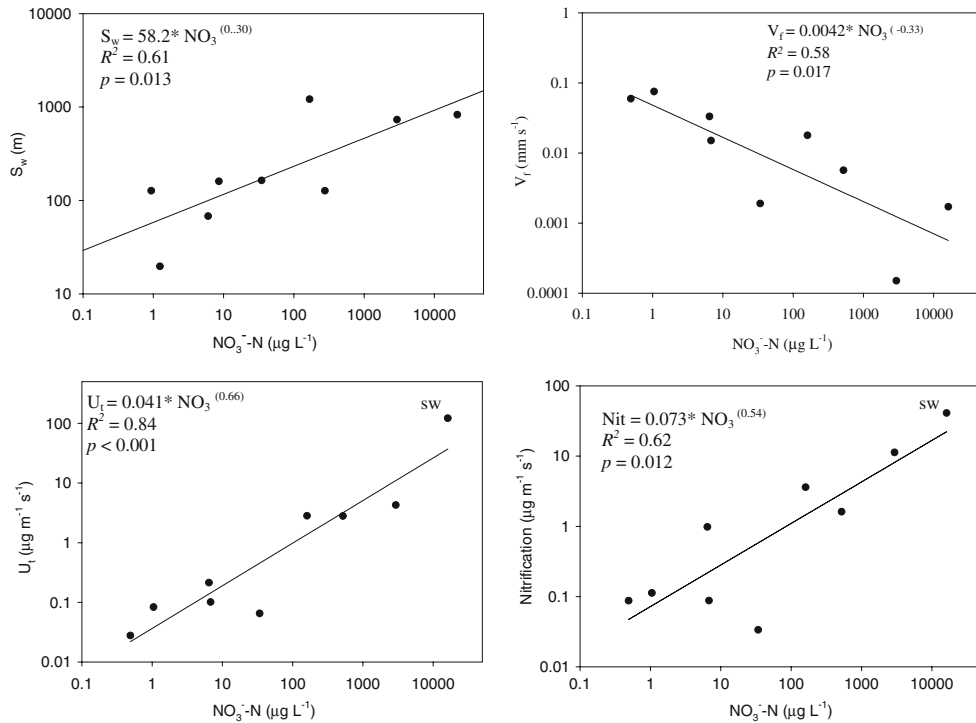


Fig. 6 Log–log relationships comparing nitrate concentrations with uptake length, uptake velocity, uptake rate, and nitrification. Data points represent averages between day

and night measurements. The nitrification and U_t data points for Swine Creek (SW) have been marked to demonstrate points with extra leverage

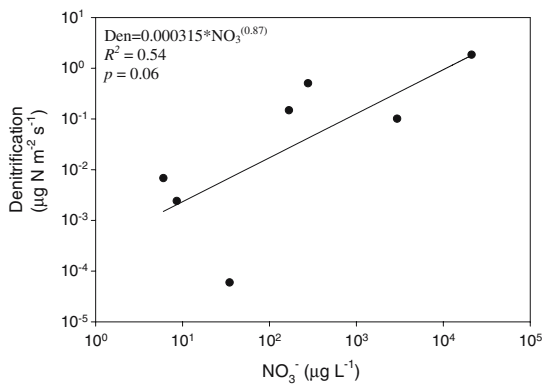


Fig. 7 Denitrification rate as a function of nitrate concentration

created by human activities, and to characterize saturation according to three potential models. We found that increased NO_3^- concentrations in the streams resulted in a stimulation of NO_3^- cycling rates and did not result in clear saturation of Michaelis–Menten form.

The 1st order model describes a relationship in which biological process rates are directly proportional to N concentration and will increase linearly with N concentration. The exponent (slope) of the increases in U_t and nitrification were less than one, which did not support the 1st order model. Also, S_w increased and V_f decreased as a function of NO_3^- concentration, which indicated that N spiraling was not following 1st order function across streams. Conversely, the relationship between denitrification and NO_3^- concentration did meet the criteria for the 1st order model.

According to the concept of saturation, NO_3^- concentration would reach a level at which biological capacity is saturated, and beyond which additional NO_3^- would no longer stimulate increased cycling, however, U_t , nitrification, and denitrification showed no sign of saturation ($K_s \gg$ experimental concentrations). Also if saturation were occurring as predicted by the Michaelis–Menten model, S_w would be expected to exhibit a linear relationship with increasing NO_3^- concentration

(Fig. 1), which was not found to be true. The data from our study do not support the hypothesis of Michaelis–Menten saturation across streams as Bernot and Dodds (2005) had predicted.

Alternatively, according to an Efficiency Loss response, process rates of N cycling will increase with NO_3^- concentration, but at a slower rate than the increase in N concentration, resulting in a loss of N processing efficiency. Across the nine streams investigated, increases in U_t and nitrification were consistent with the Efficiency Loss model. Also as predicted by this model, V_f decreases along the NO_3^- gradient and S_w continued to increase with increasing NO_3^- concentration. Therefore, data from our study support the concept of Efficiency Loss response, in which the efficiency of N processing decreases with the increase in NO_3^- availability.

The results presented here represent the response to increased NO_3^- concentrations across a spatial gradient of streams receiving a presumably steady, chronic level of N input. This response may differ from responses to acute pulses of NO_3^- concentration, which may not follow the same pattern observed here. Dodds et al. (2002) reported a 1st order response to short NO_3^- additions on Kings Creek, while O'Brien (2006) observed saturation of NO_3^- uptake in response to short-term addition experiments in three prairie streams. Thus the response of an individual stream to temporal increases in NO_3^- may follow the Michaelis–Menten or 1st order models, but the response across streams with chronic NO_3^- inputs is best described with the Efficiency Loss model.

We hypothesize that diverse microbial communities that are exposed to elevated levels of NO_3^- over longer periods of time adjust to higher NO_3^- concentrations. This adjustment may occur as a result of changes in biochemical pathways, changes in microbial biomass or changes in community composition. Whereas short-term response to increased NO_3^- could be more likely to follow Michaelis–Menten type saturation, long-term response of the microbial community leads to the Efficiency Loss response we observed in this study. Further research is necessary to establish the exact mechanism for this form of saturation across a variety of stream types.

Denitrification and N_2O production

The increase in denitrification with NO_3^- concentration was consistent with a 1st order model across streams and did not show signs of saturation. Few studies have looked at the saturation kinetics of denitrification across whole streams. Denitrification rates saturate in laboratory experiments, with a wide range of half-saturation coefficients (K_s 180–8,900 $\mu\text{g l}^{-1}$) across a river continuum (Garcia-Ruiz et al. 1998). Kemp and Dodds (2002b) found that denitrification did not always saturate in prairie stream sediments, and predicted a linear response between denitrification rates and NO_3^- in their scaled ecosystem estimates.

Denitrification rate may eventually saturate at very elevated NO_3^- , although this was not detected by our current study. Bernot and Dodds (2005) predicted saturation rates of 100–500 $\text{mg N m}^{-2} \text{ day}^{-1}$. Only the denitrification rate observed in Swine Creek fell into this range. Denitrification is also highly variable within streams, as well as across streams, and NO_3^- concentration is certainly not the only controlling factor. Other factors influencing the rate of denitrification include the availability of labile carbon, dissolved oxygen availability, and microbial biomass (Cook and White 1987). All of these factors also directly influence community respiration.

Denitrification rates were considerably less than uptake and nitrification within each stream, and usually comprised about 1% of U_t . Denitrification was only a significant sink for NO_3^- in one stream (Wal-Mart Ditch). These results are similar to the findings of Royer et al. (2004), who observed that measured denitrification rates (which ranged from <2.4 to 360 $\text{mg m}^{-2} \text{ day}^{-1}$) were much slower than commonly observed U_t leading to denitrification lengths (distance required for the average molecule of NO_3^- to be denitrified) substantially longer than S_w .

If the slope between log denitrification and log NO_3^- was greater than the slope of log U_t regression, then denitrification would become more important relative to U_t as NO_3^- concentration increased. Although the slope between log denitrification and log NO_3^- was not significantly different than one, it also could not be signifi-

cantly differentiated from the slope of the U_t regression. Therefore, we are unable to determine if denitrification became more important relative to uptake as NO_3^- concentration increased.

Although denitrification was a small part of total NO_3^- uptake, an average of 20% of stream water NO_3^- per km in the water column was lost to denitrification while the median was 3% (Table 4). The average was heavily skewed by the relatively high rate of denitrification at Wal-Mart Ditch (90% per km), and was highly variable among streams. If Wal-Mart Ditch is excluded from the analysis, the average of the remaining eight streams was 11% of stream water NO_3^- flux lost per km to denitrification. This measurement of denitrification is limited to the removal of stream water NO_3^- and may miss denitrification that is closely linked to nitrification in the sediments. Our measurements may, therefore, underestimate the total rate of denitrification in the streams.

Production of N_2O by streams could be important because N_2O is a powerful greenhouse gas. N_2O production can be a byproduct of nitrification and denitrification. Production of isotopically labeled $^{15}\text{N}_2\text{O}$ measured in this study was considered to be primarily a product of denitrification, because NO_3^- was much more labeled than NH_4^+ . Still, the possibility exists that nitrification may have contributed to some portion of the observed $^{15}\text{N}_2\text{O}$. Our results indicate that N_2O production increased linearly with NO_3^- concentration along the NO_3^- gradient. This increase in overall N_2O production did not result from a change in ratio of $\text{N}_2:\text{N}_2\text{O}$ production by the microbial community, rather from a simple overall increase in the rate of denitrification. These data suggest that production of N_2O in streams will increase with NO_3^- concentrations and may contribute to greenhouse gas emissions, although more extensive studies will be necessary to confirm this.

Our ability to detect denitrification was limited by appearance ^{15}N label in dissolved N_2 or N_2O in a pattern that was conducive to modeling. Although the $\delta^{15}\text{N}$ of N_2 gas during the plateau was higher than background in K2A and Shane Creek, there was no discernable pattern to the longitudinal flux data, thus any estimate of denitrification from these data would be highly questionable. Minimum limits of detection for

denitrification were difficult to establish, because of a lack of $^{15}\text{N}_2$ flux pattern in these streams, probably related to rapid reaeration and slow denitrification rate. These streams were had NO_3^- concentrations in the water column that were just above detection, so we presume rates were low.

Nitrification

Although nitrification was historically thought to be important only in streams with relatively high ammonium concentrations, our data suggest that nitrification provides an important source of NO_3^- in streams. Some research suggests that nitrification may be important in low-nutrient freshwater systems (Dodds and Jones 1987), but it was not widely appreciated until recently that nitrification could be an important flux in relatively pristine streams (e.g., Peterson et al. 2001; Kemp and Dodds 2002a).

The benefit of whole-stream NO_3^- isotope releases was that they showed that dilution of $^{15}\text{NO}_3^-$ that was not directly accounted for by groundwater dilution must be caused by nitrification. We measured significant nitrification even in our lowest- NO_3^- streams. Furthermore, uptake of NO_3^- was well correlated to nitrification rates (Fig. 4), suggesting that NO_3^- availability via nitrification influences uptake rates, at least over the short term. This coupling of nitrification and uptake confirms and extends the patterns observed by Kemp and Dodds (2002a) for four lower NO_3^- streams.

Biological N demand

One possible explanation for the lack of Michaelis–Menten saturation is that biological N demand also increased along the nutrient gradient. However, total biotic N demand calculated from the whole-stream metabolism estimates did not support this idea. Total biotic N demand did not co-vary with the NO_3^- gradient or with U_t (Fig. 8). Several assumptions were used to calculate assimilatory demand, so this comparison should be viewed with caution.

Increase in ^{15}N of the biomass collected from each stream is another piece of evidence that could potentially explain the increase in U_t along the

gradient of NO_3^- concentration (Fig. 8), but biomass ^{15}N assimilation did not correlate with U_t , NO_3^- concentration, standing-stock of organic matter, or whole-stream metabolism. The lack of continuity between the observed assimilatory uptake in the biomass and the other measures of uptake may be due to the inherent errors associated with scaling these measurements up to the whole stream.

This decoupling of rate of label entering individual ecosystem compartments from concentration of NO_3^- in the water column is most likely due to the difficulties of scaling up small-scale measurements, such as those used to estimate ^{15}N assimilation, to ecosystem level (Schindler 1998). Heterogeneity in spatial distribution of stream biota and NO_3^- uptake by the biota made accurate estimates of NO_3^- incorporation into the biomass difficult due to the large number of samples required. A more intense sampling regime may be required to better quantify ^{15}N assimilated into stream biomass. Because of the reasons listed above, we consider U_t to be a more accurate estimate of whole-stream uptake than biomass ^{15}N assimilation scaled to the whole stream.

Wal-Mart Ditch

Being the most extreme example of a human-impacted stream of those we studied, Wal-Mart Ditch (a concrete ditch) merits its own explanation as to how it fits in the continuum of streams investigated in this study. Wal-Mart Ditch was an

exceptionally wide and shallow “stream” relative to its discharge, which led to a large degree of interaction between the biota and the water column. The stream biota was a highly active, 0.5 cm thick, gelatinous biofilm consisting of diatoms and cyanobacteria at the time of our experiment. The concentration of NO_3^- was $670 \mu\text{g l}^{-1}$ at the head of the reach, and reduced to $<10 \mu\text{g l}^{-1}$ after only 300 m by the highly active biofilm. Much of this reduction in NO_3^- concentration was attributable to assimilation. The high primary production, respiration, and NO_3^- uptake in the Wal-Mart Ditch were similar to those of the concrete-lined stream documented by Kent et al. (2005).

During nighttime hours, the decrease in NO_3^- concentration along the stream reach was much less and was primarily attributable to denitrification. During the day, the biofilm was highly autotrophic, leading to rapid assimilation of available NO_3^- , while resulting in the release of large quantities of dissolved and particulate organic N. As a result, the quantity of N leaving the reach as organic N exceeded the amount of dissolved inorganic N assimilated in the stream reach. Thus, during the day, the stream did not serve as an N sink as the NO_3^- data suggest. At night, respiration from the biofilm was enormous, resulting in a rapid drop in O_2 concentration. It is very likely that large portions of the biofilm went anoxic and facilitated denitrification. Inclusion or exclusion of this site from the cross-stream analysis did not greatly alter the conclusions or model fits.

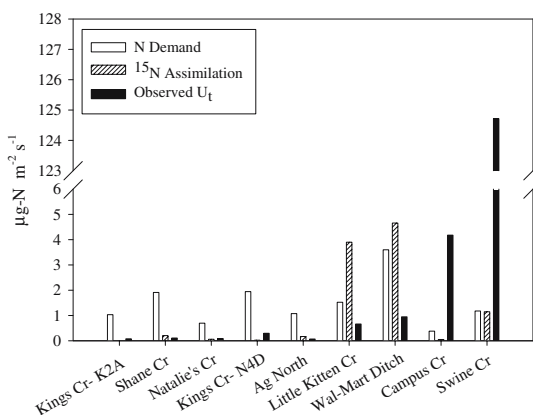


Fig. 8 Biotic N demand and assimilatory nitrate uptake in the streams investigated

Conclusions

The relationship of N processing to stream water NO_3^- concentration did not saturate according to our hypothesis, rather, it conformed to an Efficiency Loss model in which the efficiency at which N is cycled and retained decreases with increasing nutrient concentration. In low- NO_3^- streams, available NO_3^- was spiraled very quickly and traveled a relatively short distance before being taken up again. As the concentration of NO_3^- increased, the magnitude and length of spiraling also increased. Although the rate of cycling between organic and inorganic forms increased along the NO_3^- gradient,

the relative proportion of NO_3^- retained by the stream decreased, resulting in longer uptake lengths and a lower V_f .

For the most part, denitrification was a minor flux in relation the rapid rate of turnover of water column NO_3^- , composing only ~1% of U_t . Denitrification may remove a significant percent of the stream water NO_3^- over longer distances, with an average removal of $20\% \text{ km}^{-1}$ across all nine streams, although this was highly variable and removal in a majority of the streams was $<5\% \text{ km}^{-1}$. The relative importance of both groundwater input and denitrification decreased along the gradient. NO_3^- flux increased faster, relative to increases in process fluxes characterized by an exponential decrease in the amount of N processed relative to N available. Overall NO_3^- retained by the stream reach, as a proportion of influx, decreased with increasing NO_3^- concentration.

This study demonstrates that NO_3^- turns over rapidly in stream water, even in streams with high nitrate loads, leading to short-term retention. The rate of turnover declines with concentration. Although some streams demonstrate significant denitrification over long distances, most only showed modest NO_3^- removal ($5\% \text{ km}^{-1}$). These results have implication toward the management of nutrient export from the landscape. First, longer streams will have a greater effect on nitrate retention and removal. Management strategies that involve reducing channel length (i.e. channelizing and straitening streams) should be avoided. Efforts should also be directed toward reducing N loads prior to reaching the stream, through the protection of wetlands and riparian areas.

Acknowledgements We thank Eric Banner, Christa Carlson, Joey Dodds, Katie Gleason, Dolly Gudder, Brian Monser, Rosemary Ramundo, Alyssa Standorf, and Mandy Stone for field and laboratory assistance. We thank the LINX II Research Group for developing the protocols used in this study. We thank Steve Hamilton for providing the protocols and exetainers for dissolved gas analysis, and the subsurface sippers. We also thank Rich Scheibly for his assistance with the transient storage modeling. Dolly Gudder and the LAB aquatic journal club provided helpful comments on this manuscript. The project was funded by the National Science Foundation (project #DEB-0111410) as part of the Lotic Intersite

Nitrogen eXperiment (LINX II), Konza LTER, NSF-EPSCOR. This is publication # 06-183-J of the Kansas Agricultural Experimental Station.

References

- American Public Health Association (APHA) (1995) Standard methods for the examination of water and wastewater. American Public Health Association, Washington, DC
- Alexander RB, Smith RA, Schwarz GE (2000) Effect of stream channel size on the delivery of nitrogen to the Gulf of Mexico. *Nature* 403:758–761
- Bernhardt ES, Likens GE, Hall RO, Buso DC, Fisher SG, Burton TM, Meyer JL, McDowell MH, Mayer MS, Bowden WB, Findlay S, MacNeale KH, Stelzer RS, Lowe WH (2005) Can't see the forest for the stream? In-stream processing and terrestrial nitrogen exports. *Bioscience* 55:219–230
- Bernot MJ, Dodds WK (2005) Nitrogen retention, removal and saturation in lotic ecosystems. *Ecosystems* 8:442–453
- Bothwell ML (1989) Phosphorous limited growth dynamics of lotic periphytic diatom communities—areal biomass and cellular growth rate responses. *Can J Fish Aquat Sci* 46:1293–1301
- Bott TL (1996) Primary productivity and community respiration. In: Hauer FR, Lamberti GA (ed) *Methods in stream ecology*. Academic Press, San Diego
- Cook JG, White RE (1987) Spatial distribution of denitrifying activity in a stream draining an agricultural catchment. *Freshw Biol* 18:509–519
- Dodds WK (1995) Availability, uptake and regeneration of phosphate in mesocosms with varied levels of P deficiency. *Hydrobiologia* 297:1–9
- Dodds WK, Jones RD (1987) Potential rates of nitrification and denitrification in an oligotrophic freshwater sediment system. *Microb Ecol* 14:91–100
- Dodds WK, Oakes RM (2004) A technique for establishing reference nutrient concentrations across watersheds impacted by humans. *Limnol Oceanogr Meth* 2:333–341
- Dodds WK, Welch EB (2000) Establishing nutrient criteria in streams. *J N Am Benthol Soc* 19:186–196
- Dodds WK, Evans-White MA, Gerlanc N, Gray L, Gudder DA, Kemp MJ, López AJ, Stagliano D, Strauss E, Tank JL, Whiles MR, Wollheim W (2000) Quantification of the nitrogen cycle in a prairie stream. *Ecosystems* 3:574–589
- Dodds WK, López AJ, Bowden WB, Gregory S, Grimm NB, Hamilton SK, Hershey AE, Martí E, McDowell WB, Meyer JL, Morrall D, Mulholland PJ, Peterson BJ, Tank JL, Vallett HM, Webster JR, Wollheim W (2002) N uptake as a function of concentration in streams. *J N Am Benthol Soc* 21:206–220
- Dodds WK, Gido K, Whiles M, Fritz K, Mathews W (2004) Life on the edge: ecology of Great Plains prairie streams. *Bioscience* 54:207–281

- Garcia-Ruiz R, Pattinson SH, Whitton BA (1998) Kinetic parameters of denitrification in a river continuum. *Appl Environ Microbiol* 64:2533–2538
- Graham JM, Krazenfelder JA, Auer MT (1985) Light and Temperature as factors regulating seasonal growth and distribution of *Ulothrix zonata* (Ulvophyceae). *J Phycol* 21:228–234
- Gray L, Dodds WK (1998) Structure and dynamics of aquatic communities. In: Knapp AK, Briggs JM, Hartnett DC, Collins SL (eds) *Grassland dynamics: long-term ecological research in tallgrass prairie*. Oxford University Press, New York
- Gray L, Macpherson GL, Koelliker JK, Dodds WK (1998) Hydrology and aquatic chemistry. In: Knapp AK, Briggs JM, Hartnett DC, Collins SL (eds) *Grassland dynamics: long-term ecological research in tallgrass prairie*. Oxford University Press, New York
- Hensel DR and Hirsch RM (2002) *Statistical methods in water resources. Techniques of water resources investigations, Book 4 Chapter A3*. United States Geological Survey, Washington
- Hill AR (1979) Denitrification in the nitrogen budget of a river ecosystem. *Science* 281:291–292
- Hill WR, Mulholland PJ, Marzolf ER (2001) Stream ecosystem responses to forest leaf emergence in spring. *Ecology* 82:2306–2319
- Inwood SE, Tank JL, Bernot MJ (2005) Patterns of denitrification associated with land use in 9 midwestern headwater streams. *J N Am Benthol Soc* 24:227–245
- Kemp MJ, Dodds WK (2002a) Comparisons of nitrification and denitrification in pristine and agriculturally influenced streams. *Ecol Appl* 12:998–1009
- Kemp MJ, Dodds WK (2002b) The influence of ammonium, nitrate, and dissolved oxygen concentration on uptake, nitrification, and denitrification rates associated with prairie stream substrata. *Limnol Oceanogr* 47:1380–1393
- Kent R, Belitz K, Burton CA (2005) Algal productivity and nitrate assimilation in an effluent dominated concrete lined stream. *J Am Wat Res Assoc* 41:1109–1128
- Lewis WM (2002) Yield of nitrogen from minimally disturbed watersheds of the United States. *Biogeochemistry* 57:375–385
- Mulholland PJ (2004) The importance of in-stream uptake for regulating stream concentrations and outputs of N and P from a forested watershed: evidence from long-term chemistry records for Walker Branch Watershed. *Biogeochemistry* 70:403–426
- Mulholland PJ, Steinman AD, Elwood JW (1990) Measurements of phosphorous uptake length in streams—comparison of radiotracer and stable PO_4 releases. *Can J Fish Aquat Sci* 47:2351–2357
- Mulholland PJ, Valett HM, Webster JR, Thomas SA, Cooper LW, Hamilton SK, Peterson BJ (2004) Stream denitrification and total nitrate uptake rates measured using a field N-15 tracer addition approach. *Limnol Oceanogr* 49:809–820
- Niyogi DK, Simon KS, Townsend CR (2004) Land-use and stream ecosystem functioning: nutrient uptake in streams that contrast in agricultural development. *Arch Hydrobiol* 180:471–486
- O'Brien JM (2006) Controls of nitrogen spiraling in Kansas streams. PhD Dissertation, Kansas State University
- O'Brien JM, Williard KWJ (2006) Potential denitrification rates in a agricultural stream in southern Illinois. *J Freshw Ecol* 21:157–162
- Oviatt CG (1998) Geomorphology of Konza Prairie. In: Knapp AK, Briggs JM, Hartnett DC, Collins SL (eds) *Grassland dynamics: long-term ecological research in tallgrass prairie*. Oxford University Press, New York
- Peterson BJ, Wollheim W, Mulholland PJ, Webster JR, Meyer JL, Tank JL, Grimm NB, Bowden WB, Vallet HM, Hershey AE, McDowell WB, Dodds WK, Hamilton SK, Gregory S, D'Angelo DJ (2001) Control of nitrogen export from watersheds by headwater streams. *Science* 292:86–90
- Rabalais NN (2002) Nitrogen in aquatic ecosystems. *Ambio* 31:102–111
- Rathbun RE, Stephens DW, Shultz DJ, Tai DY (1978) Laboratory studies of gas tracers for reaeration. *P Am Soc Civil Eng* 104:215–229
- Royer TV, Tank JL, David MB (2004) Transport and fate of nitrate in headwater agricultural streams in Illinois. *J Environ Qual* 33:1296–1304
- Schindler DW (1998) Replication versus realism: the need for ecosystem-scale experiments. *Ecosystems* 1:323–334
- Sigman DM, Altabet MA, Michener R, McCorkle DC, Fry B, Holmes RM (1997) Natural abundance-level measurement of nitrogen isotopic composition of oceanic nitrate: an adaptation of the ammonia diffusion method. *Mar Chem* 57:227–242
- Stream Solute Workshop (1990) Concepts and methods for assessing solute dynamics in stream ecosystems. *J N Am Benthol Soc* 9:95–119
- Tank JL, Dodds WK (2003) Responses of heterotrophic and autotrophic biofilms to nutrients in ten streams. *Freshw Biol* 48:1031–1049
- Torrecilla NJ, Galve JP, Zaera LG, Retarnar JF, Alvarez ANA (2005) Nutrient sources and dynamics in a Mediterranean fluvial regime (Ebro River, NE Spain) and their implications for water management. *J Hydrol* 304:166–182
- Valderrama JC (1981) The simultaneous analysis of total nitrogen and phosphorus in natural waters. *Mar Chem* 10:109–122
- Webster JR, Ehrman TP (1996) Solute dynamics. In: Hauer FR, Lamberti GA (eds) *Methods in stream ecology*. Academic Press, San Diego
- Webster JR, Patten BC (1979) Effects of watershed perturbations on stream potassium and calcium dynamics. *Ecol Monogr* 49:51–72
- Webster JR, Mulholland PJ, Tank JL, Valett HM, Dodds WK, Peterson BJ, Bowden WB, Dahm CN, Findlay S, Gregory SV, Grimm NB, Hamilton SK, Johnson SL, Martí E, McDowell WH, Meyer JL, Morrall DD, Thomas SA, Wollheim WM (2003) Factors affecting ammonium uptake in streams—an inter-biome perspective. *Freshw Biol* 48:1329–1352
- Wetzel RG, Likens GE (2000) *Limnological analysis*, 3rd edn. Springer-Verlag, Berlin